ENVIRONMENTAL RESEARCH
LETTERS

Long-term climatic change and sustainable ground water resources management

To cite this article: Hugo A Loáiciga 2009 *Environ. Res. Lett.* **4** 035004

Environ. Res. Lett. 4 (2009) 035004 (11pp) doi:10.1088/1748-9326/4/3/035004

Long-term climatic change and sustainable ground water resources management

Hugo A Loáiciga

Department of Geography/UCSB, Santa Barbara, CA 93117, USA

E-mail: hugo@geog.ucsb.edu

Received 28 January 2009
Accepted for publication 14 May 2009
Published 11 August 2009
Online at stacks.iop.org/ERL/4/035004

Abstract
Atmospheric concentrations of greenhouse gases (GHGs), prominently carbon dioxide (CO_2), methane (CH_4), nitrous oxide (N_2O), and halocarbons, have risen from fossil-fuel combustion, deforestation, agriculture, and industry. There is currently heated national and international debate about the consequences of such increasing concentrations of GHGs on the Earth's climate, and, ultimately, on life and society in the world as we know it. This paper reviews (i) long-term patterns of climate change, secular climatic variability, and predicted population growth and their relation to water resources management, and, specifically, to ground water resources management, (ii) means available for mitigating and adapting to trends of climatic change and climatic variability and their impacts on ground water resources. Long-term (that is, over hundreds of millions of years), global-scale, climatic fluctuations are compared with more recent (in the Holocene) patterns of the global and regional climates to shed light on the meaning of rising mean surface temperature over the last century or so, especially in regions whose historical hydroclimatic records exhibit large inter-annual variability. One example of regional ground water resources response to global warming and population growth is presented.

Keywords: climate change, global warming, greenhouse gases, water resources, ground water.

1. Introduction

Few topics attract as much attention today as 'global warming' does. The latter term has become synonymous with the increasing trend of the Earth's mean surface temperature (defined as the average of near-surface air temperature over land and sea surface temperature) observed over the last century, and, more noticeably, post 1950. A position on the causes of global warming so defined and its probable consequences on the world's population and the global environment has been summarized in the United Nations' 2007 Intergovernmental Panel on Climate Change (IPCC) report. The IPCC (2007) report stated that human activities (mainly fossil-fuel combustion, deforestation, agriculture, industry) since the onset of the Industrial Revolution (circa 1750) have raised the atmospheric concentrations of GHGs above those that would be expected by natural causes alone. Furthermore, the IPCC (2007) report stated with very high confidence that human activities since 1750 have raised the global mean surface temperature above the level that would be expected by natural warming that followed after the last ice age. Besides the central role that mean surface temperature has on terrestrial and oceanic organisms and on essential physical and chemical environmental processes, the IPCC (2007) report cites heightened sea level rise and the melting of ice and snow as effects of global warming inferred from observations worldwide. Many other effects of global warming are identified or implied with various degrees of confidence in the IPCC (2007) report, among them changes in regional precipitation and evaporation.

Global warming driven changes in regional precipitation and evaporation have direct consequences on hydrologic processes and water resources (rivers, lakes, aquifers, wetlands, springs) through their possible shifts of basin-wide water balances. Recall the water-balance equation at the river basin or aquifer spatial scales, in which the change in water storage ΔS during an arbitrary time interval (Δt) is determined by the magnitude of the water fluxes affecting storage, namely, precipitation (P), evapotranspiration (ET), runoff (surface plus subsurface), and net human withdrawal (D):

$$\frac{\Delta S}{\Delta t} = P - \mathrm{ET} - Q - D. \qquad (1)$$

Changes on the regional water balance effected by global warming, climate-modified P and ET would trigger shifts (represented by the symbol δ) in all the terms appearing in equation (1):

$$\delta\left(\frac{\Delta S}{\Delta t}\right) = \delta P - \delta\mathrm{ET} - \delta Q - \delta D. \qquad (2)$$

Equation (2) suggests that a warming climate could trigger a complex and interrelated set of changes in water storage, precipitation, evapotranspiration, runoff, and net human withdrawal that would affect all aspects of human activity and water-related environmental processes by offsetting water availability (expressed as δP–δET, say, for plants, or δQ for aquatic organisms, or as δD for human consumption or agriculture). A voluminous body of literature has been produced over the last 30 years on a variety of examples of hydrologic change embodied by equation (2), see, for example, a review of global warming and the hydrologic cycle (Loáiciga *et al* 1996, Loáiciga 2003), global-scale predictions of water resources change driven by global warming and population change (Vörösmarty *et al* 2000), continental-scale predictions of hydrologic change (de Witt and Stankiewicz 2006), detection of global changes in runoff (Milliman *et al* 2008), and overall reviews of global warming–human–environment interactions (Houghton 2004, IPCC 2007).

The current state of long-range climate prediction (say, 100 years hence) is beset by the complexity of the Earth–atmosphere system's response to heightened post-1750 concentrations of GHGs (see, Hansen *et al* 2005) and by the uncertain nature of human adaptation to global warming, which, in turn, may affect future concentrations of GHGs (Crowley 2008, Pielke 2008). The latter statement takes greater relevance in judging the accuracy of long-range predictions of regional (say, at the river basin or aquifer spatial scales, Arnell *et al* 2003, Pielke 2008) climatic change. Figure 1 exemplifies the sensitivity of climate evolution to small differences in initial conditions. Global mean surface temperature data were fitted by Tsonis (1991) with an autoregressive model, which was then used to simulate temperature departures from the historical mean through year 2100.

Two time series of temperature departures were simulated and are shown in figure 1, the only difference between the simulated time series being a 1% difference in the initial condition used to start the simulations. Notice that the two simulated time series in figure 1 diverge from each other in magnitude and timing of lows and highs after about 40 years of simulation.

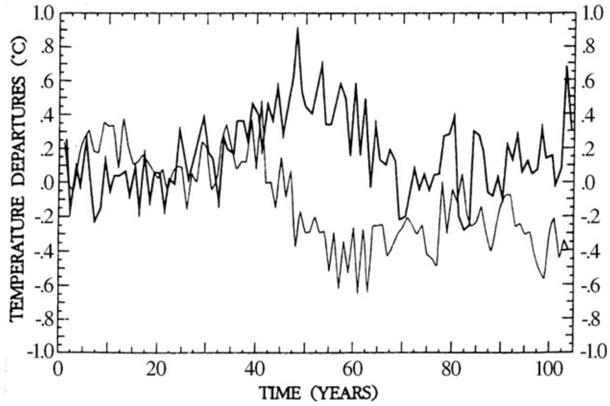

Figure 1. Divergence of two mean surface temperatures after 40 years of simulation. The initial temperatures differ by 1%. After Tsonis (1991).

Long-term, transient, simulations of the Earth's climate with coupled atmosphere–ocean general circulation models (AOGCMs) are not immune to the sensitivity of climate prediction to initial conditions (akin to the so-called 'butterfly effect' of weather prediction, see Lorenz 1964). To compound matters, AOGCMs, by necessity, parameterize and simplify their abstract representations of actual climatic feedbacks involving coupled atmospheric, oceanic, and terrestrial processes (Loáiciga *et al* 1996, Grassi 2000, Forest *et al* 2002, Roe and Baker 2007, Pielke 2008). On the other hand, one must not overlook the fact that there have been advances over the last decade in the predictive capability of AOGCMs. The IPCC (2007) report based its climate prediction on the best climate models currently available. The uncertainty of climate predictions' notwithstanding, the IPCC (2007) report called for pronounced reduction of GHGs to avert what the IPCC (and others) consider a serious threat of irreversible damage to the global environment and society. According to this precautionary principle, lack of full scientific certainty may not be used to postpone cost-effective action to prevent deleterious impacts from global warming. Nationally and internationally, the search for means to transition to a vigorous world economy less dependent on fossil fuels continues.

The world's water resources are impacted by global warming in a complex manner associated with the changes in storage and fluxes written in equation (2). Also, since the emergence of agriculture circa 10 000–15 000 years before present, the ensuing population growth has had immense cumulative impacts on the world's fresh water resources, both quantitatively and qualitatively (see, e.g., Postel *et al* 1996, Falkenmark 1997, Oki and Kane 2006, Barnett *et al* 2008). Population growth worldwide suggests that people's pressure on natural and water resources will continue for the foreseeable future, giving rise to challenges on ways to meet growing demands for potable water and better sanitation of populated areas, and for water supply to sustain economic growth while avoiding environmental degradation (Cohen 1995, Falkenmark 1997). Figure 2 graphs forecasts of the world's population through year 2050, and similarly for the United States, China and India, the first country having the

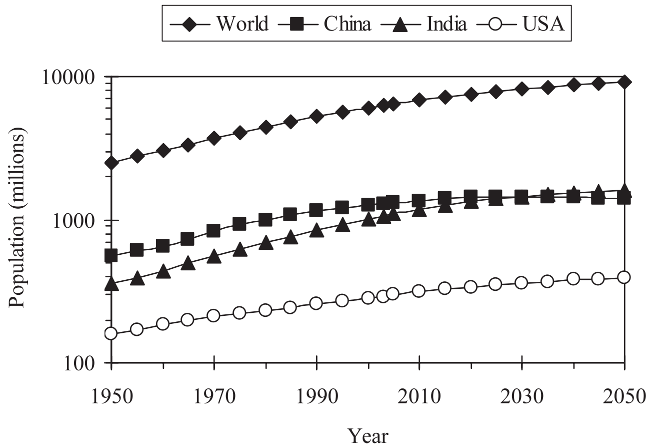

Figure 2. Population growth worldwide and in selected countries through year 2050. (Source: United Nations).

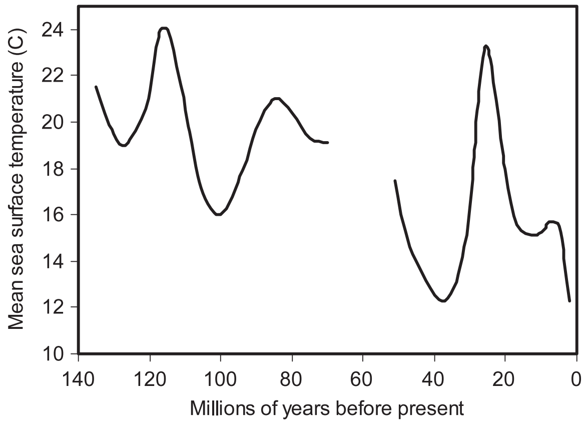

Figure 3. Mean sea surface temperature in the northern mid-latitudes (after Budyko 1977). The gap about 65 millions years before present coincides with the Cretaceous–Tertiary (K–T) boundary and the meteoric impact theorized to have occurred then.

world's largest economy and the latter two featuring the fastest growing economies among developing countries. The world population is predicted to be near 10 billion people by 2050, most of it to take place in developing countries with inadequate infrastructure and institutions overseeing water supply and sanitation. Given the reality of population growth and the tepid improvement of water systems to cope with it, the United Nations Development Program's Millennium Development Goal of reducing by one half the number of people without access to potable water and basic sanitation by 2015 appears elusive. Ground water is currently and will continue to be an important part of the world's freshwater supply (Shiklomanov and Rodda 2003, Gleick 2004).

The growing demands for water associated with population growth are intimately related to the increase in energy use required to support rising living standards worldwide and dynamic economies. In view of the immediate growing demands for water and energy (perhaps more aptly jointly called 'watergy'), the transition to a thriving world economy less dependent on fossil fuels poses enormous challenges (Hardin 1993).

The remainder of this paper is organized in three sections. First, a review of climate change and atmospheric CO_2 evolution over geologic time is presented alongside with measurements of hydroclimatic data made since the early 1900s in a region of special interest in this work. Section 3 describes a method available for assessing likely changes in ground water resources in a 2 × CO_2-world, that is, one in which atmospheric CO_2 concentration is twice that of a baseline year (1 × CO_2 concentration), taken to be that of 1990 (approximately 360 ppmv) by the Kyoto Protocol for climate-change control (Houghton 2004). Section 4 shows an application of the method for climate-change prediction to develop courses of action for managing a regional ground water resource. Generalizations of the concepts and methods of this paper are made as needed to point directions along which—according to this author's opinion—rest some of the best opportunities to mitigate and adapt to continuing climate change.

This paper summarizes the author's work on climate change/variability and ground water resources sustainability. Its contribution lies in the synthesis of that work with other pertinent publications by several researchers in the same or related fields.

2. Is the Earth warming?

2.1. The Earth's surface temperature

Figure 3 shows the fluctuation of the mean sea surface temperature (used as a proxy for the lower-atmosphere temperature) in the northern mid-latitudes during the last 140 million years according to a reconstruction by Budyko (1977). There is gap in the reconstruction shown in figure 3 in the period surrounding the Cretaceous–Tertiary boundary (circa 65 million years before present), contemporaneous with the theorized meteorite impact on Earth that, among other effects, might have caused the extinction of the dinosaurs.

Figure 3 shows pronounced fluctuations of the mean surface temperature over geologic time, and, overall, a long-term decline in mean surface temperature. It can be inferred from figure 3 that the lower-atmosphere temperature in the northern mid-latitudes has decreased about 10 °C in the last 140 million years.

The pattern of lower-atmosphere temperature during the second half of the Pleistocene (started 1 million years ago and ended with the start of the Holocene about 10 000 years ago) shown in figure 4 supplements the longer-term temperature history of figure 3. Figure 4 shows the minimum lower-atmosphere temperature during the ice ages that occurred in the last 400 000 years, reconstructed from air–temperature deviations inferred from Antarctic ice cores (Fedorov *et al* 2006) and then adjusted by this author by an approximate Holocene mean surface temperature of 15 °C. In addition, figure 4 shows the maximum lower-atmosphere temperature during interglacial periods during the last 400 000 years (see Imbrie and Imbrie 1980, for a discussion of orbital variations and climatic response).

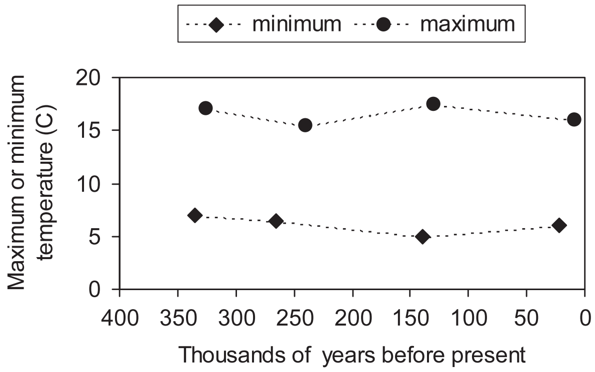

Figure 4. Minimum ice age and maximum interglacial temperatures during the last 400 000 years.

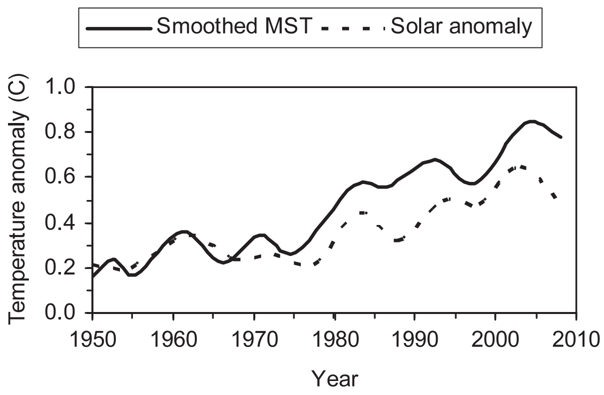

Figure 5. Mean surface temperature (smoothed MST) and solar-influenced temperature anomaly (solar anomaly) since 1950 (adapted from Scafetta and West 2008).

Figure 4 shows that the minimum and maximum temperatures associated with ice ages and interglacial periods have remained relatively steady during the second half of the Pleistocene. Current mean surface temperature—representative of interglacial warming following the last ice age—is comparable with warm interglacial temperatures of the last 400 000 years.

Figure 5 shows the smoothed global mean surface temperature (MST) anomaly since 1950 (see the solid line on figure 5). The anomaly equals the difference between the measured global surface temperature and its time average between 1890 and 1910, the period used as reference to calculate a time average of MST (Scafetta and West 2008). The anomaly-MST data were low-pass filtered to remove any volcanic signal and smoothed to highlight the influence of the 11 year solar cycle (of radiation intensity reaching Earth) on the surface temperature (Scafetta and West 2008). It is seen in figure 5 that the (smoothed) mean surface temperature increased about 0.68 °C between 1950 and 2008. Notice, however, that the mean surface temperature has decreased since 2002.

Figure 5 also shows as a dotted line the reconstructed temperature anomaly between 1950 and 2008 caused by changes in the intensity of the solar radiation reaching the Earth. The graph in figure 5 shows that the smoothed

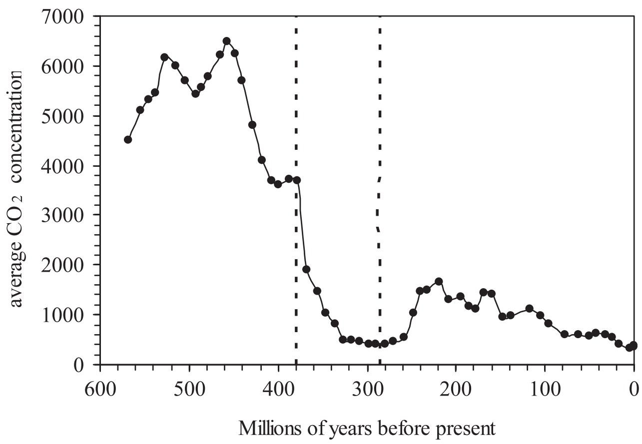

Figure 6. Average atmospheric CO_2 concentration (adapted from Berner 1997). The CO_2 concentration is in ppmv (parts per million by volume). The interval between the two vertical dotted lines define the carboniferous period, when plants absorbed much CO_2.

mean surface temperature anomaly and the solar temperature anomaly are nearly synchronous in their low and high values. The two curves in figure 5 indicate that the solar temperature anomaly accounts for about 0.44 °C of the 0.68 °C rise in the smoothed mean surface temperature anomaly, the remainder—or 0.24 °C—of the rise is caused by other phenomena, one of them being the anthropogenic buildup of GHGs in the atmosphere. The role of solar irradiance on the mean Earth's surface temperature has been interpreted in a manner different to that suggested by figure 5 by other authors (see Duffy *et al* 2009).

2.2. Atmospheric CO_2 over geologic time

Long-term average atmospheric CO_2 concentration is depicted in figure 6, adapted from Berner (1997). Evidently, there has been a substantial fluctuation of atmospheric CO_2 over geologic time, the overall trend over the last 100 million years being downwards. At the climax of the last ice age, some 25 000 years ago, atmospheric CO_2 was about 180 ppmv. By 1750 it had risen to 280 ppmv, and it is currently 385 ppmv (Fedorov *et al* 2006, Loáiciga 2006, 2007). It was a approximately 285 and 370 ppmv in 1800 and 1990, respectively. It is this increase of about 105 ppmv since the start of the Industrial Revolution (circa 1750) and the future emissions of GHGs what causes concern nowadays about possible future disruptions of the relative mild climate enjoyed during the Holocene.

The early high concentration of CO_2, in the thousands of ppmv, was caused by degassing of the Earth's crust. Part of that CO_2 was consumed through geochemical reactions on land (silicate mineral weathering) and in the ocean (formation of carbonate minerals, see Krauskopf 1979, Berner 1997, Loaiciga 2006, 2007). Some of it was fixed as plant biomass and buried in the Earth crust as fossil hydrocarbons, some of which have been recently converted into energy and GHGs through fossil-fuel combustion.

Figure 7 shows the minimum atmospheric CO_2 concentration at the climax of Pleistocene ice ages during the

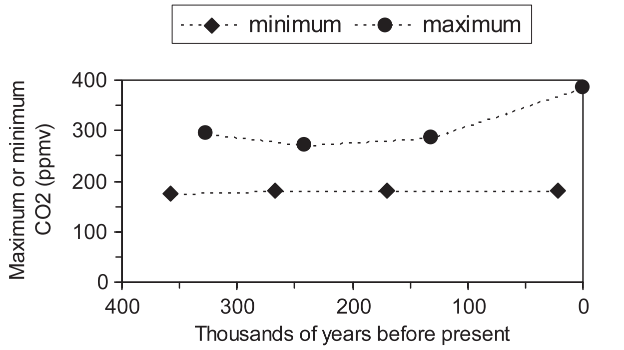

Figure 7. Minimum and maximum atmospheric CO_2 concentrations during ice ages and interglacial periods, respectively, over the last 400 000 years.

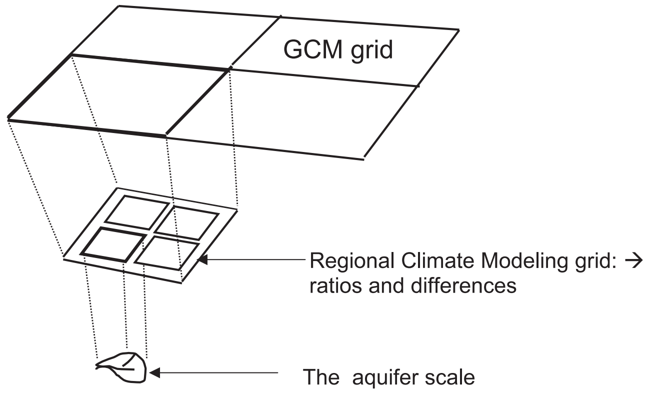

Figure 8. Diagram illustrating the downscaling from GCM to RCM to hydrologic models.

last 400 000 years reconstructed from ice cores (Fedorov *et al* 2006), as well as the maximum atmospheric CO_2 concentrations during the intervening warm interglacial periods. The minimum CO_2 concentration has stayed very close to 180 ppmv during the last 400 000 years. The maximum CO_2 concentration, on the other hand, has risen during the present warm interglacial period to 385 ppmv—or about 100 ppmv higher than those of previous interglacial periods in the Pleistocene.

The weight of the evidence from figures 3–7 is that atmospheric CO_2 concentration and mean surface temperature have exhibited anything but drastic change over geologic time. In contrast, the current warm interglacial period, the Holocene, has been characterized by a relatively mild climate globally, which has permitted the rise of humans and their industrialized society. Oddly, humans find themselves at present wondering if that advanced level of industrialization and the cumulative environmental change they have effected on Earth could modify its climate in ways that might threaten the survival of life as we know it.

As to the question of whether or not the Earth is warming, the answer is not a short phrase. The Earth has warmed between 5 and 10 °C—depending on location—since the end of the last ice age about 10 000 to 15 000 years before present (Budyko 1977, Gribbin 1979). In that time, global sea level has risen approximately 120 m (Pugh 2004). It was shown in figure 5 that since 1950 the Earth has warmed about 0.68 °C. A significant fraction of that rise may be attributable to changes in solar radiation reaching the Earth (Scafetta and West 2008; see an opposing view about this in Duffy *et al* 2009), and the exact contribution of post-Industrial Revolution GHGs anthropogenic emissions remains unsettled. Because of the complexity of the atmosphere–Earth system, with its feedbacks and the ever changing human environmental footprint, the future prediction of the Earth's climate evolution using the most advanced tools currently available—coupled atmospheric–ocean general circulation models—remains a challenge.

An approach to create 2 × CO_2 steady-state scenario of future climate under a warming Earth for the purpose of ground water management is presented next. This approach does not rely on the long-term transient simulation of the Earth's climate, thus avoiding the difficult problem of long-range prediction beset by nonlinear and uncertain (if not unknown) feedbacks of the Earth's climate system. Instead, the 2 × CO_2 steady-state scenario provides a portrait of how a regional climate might look like under doubled CO_2 atmospheric concentration using some of the best tools for climate-scenario prediction. Pros and cons of the 2 × CO_2 steady-state approach are found in section 3.

3. An approach to developing warmer-climate scenarios

Loáiciga *et al* (2000) presented a method to create 2 × CO_2 climate scenarios—in terms of regional precipitation, runoff, mean surface temperature, etc—and using these regionally averaged hydroclimatic variables to simulate ground water recharge that drives ground water flow, hydraulic head, and spring flow in a regional karst aquifer. The creation of a 2 × CO_2 climate scenario—as proposed by the National Center for Atmospheric Research's Vegetation Ecosystem Modeling and Analysis Project (NCAR-VEMAP, see, e.g., Kittel *et al* 1995)—starts with a 2 × CO_2 prediction of climate variables simulated in steady-state mode, and represented by the average outputs of six GCMs (for general circulation model, see Loáiciga *et al* 2000). The variables correspond to a doubled concentration of atmospheric CO_2 relative to a baseline, or 1 × CO_2, concentration (equal to the 1990 concentration of 360 ppmv). The 2 × CO_2 simulated variables represent averages within the cells of the spatial grid of the GCM, typically made up of coarse cells with sides of a few hundreds of kilometers long. The 2 × CO_2 variables simulated with the GCM serve as boundary conditions for a regional climate model (RCM) whose grid consists of cells with sides of a few tens of kilometers long. The use of the coarse-scale GCM-simulated variables as boundary conditions for a finer-resolution RCM, a type of downscaling technique, is illustrated in figure 8. The RCM simulates 2 × CO_2 hydroclimatic variables at its finer spatial scale and in steady-state mode, as well. The use of a reference 2 × CO_2 concentration is reasonable when the purpose is to create a scenario of climatic change relative to that corresponding to a known (historical)

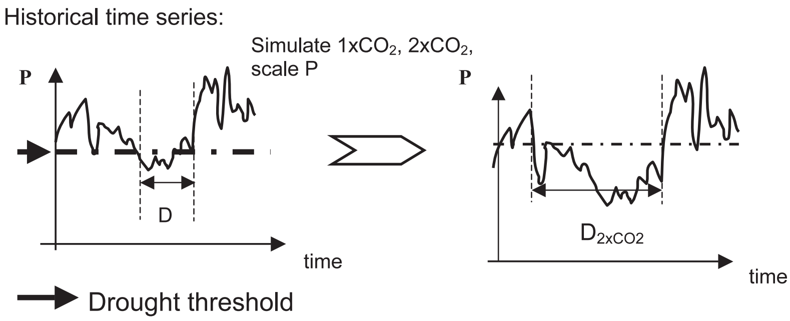

Figure 9. Diagram depicting the scaling of a precipitation time series.

$1 \times CO_2$ baseline condition. It also bypasses the difficulty of guessing what the CO_2 atmospheric evolution would be over the 21st century. Recent data presented by Crowley (2008) shows that the CO_2 emissions for years 2005–2007 do not conform to any of the IPCC (2007) emission scenarios, and, in fact, exceed the worst-case scenario A1F1 entertained by the IPCC (2007).

An average $1 \times CO_2$ baseline, steady-state, simulation of hydroclimatic variables is also obtained, which serve as boundary conditions for the RCM-based $1 \times CO_2$, steady-state, simulation of climatic variables at its finer spatial resolution. The $1 \times CO_2$ is a reference concentration, like that which prevailed in 1990 (equal to 360 ppmv) and that is used by the Kyoto Protocol to set goals to reduce GHGs concentrations. With the $1 \times CO_2$ and $2 \times CO_2$-based RCM simulations of, say, precipitation, denoted by $P_{1\times CO_2}$ and $P_{2\times CO_2}$, respectively, a ratio of precipitation $P_{2\times CO_2}/P_{1\times CO_2}$ is formed. This ratio varies from cell to cell in the RCM spatial grid. The purpose of the precipitation ratio so formed is to use it to scale historical regional precipitation (that, is from modern instrumental records), say, during wet, or dry, or normal climatic conditions.

Suppose that a time series of historical precipitation, P_H, recorded during a dry period is available. P_H is scaled by the precipitation ratio to produce a scenario of what the precipitation would be in a $2 \times CO_2$, warmer, world with dry conditions prevailing in the region of interest:

$$P_{2\times CO_2 \text{scenario}} = P_H \frac{P_{2\times CO_2}}{P_{1\times CO_2}}. \tag{3}$$

Assuming that (i) $P_{1\times CO_2}$ and $P_{2\times CO_2}$ are statistically independent between themselves and independent of P_H as well, and (ii) that $P_{1\times CO_2}$ is an unbiased estimator of P_H, taking the expected value on both sides of equation (3) shows that the mean of $P_{2\times CO_2 \text{scenario}}$ equals the mean of $P_{2\times CO_2}$, this being a desirable property of the scaled estimator of future precipitation in a warmer climate. Ratios can be so constructed for other regionally averaged variables such as runoff, evapotranspiration, etc. The scaled regional variables—akin to precipitation in equation (3)—are then used to drive basin- or aquifer-scale simulation models placed at the finest level of spatial resolution in the downscaling technique depicted in figure 8. The output from aquifer models would be ground water flow rates, hydraulic heads, spring flows, and the like, hypothesized to be representative of those to be expected in a $2 \times CO_2$ world. Figure 9 shows the effect of scaling a precipitation time series encompassing a dry period of duration D. In this example, the scaled time series is seen to exhibit a drought of longer duration and greater severity than the historical time series.

It is customary to use differences of temperature, instead of temperature ratios, to create $2 \times CO_2$ surface temperature scenarios:

$$T_{2\times CO_2 \text{scenario}} = \{T_{2\times CO_2} - T_{1\times CO_2}\} + T_H \tag{4}$$

in which $T_{1\times CO_2}$ and $T_{2\times CO_2}$ are the baseline CO_2 and double-CO_2 GCM-simulated time series, and T_H denotes the historical time series of temperature. Assuming that $T_{1\times CO_2}$ is an unbiased estimator of T_H, taking the expected value in equation (4) shows that the mean of $T_{2\times CO_2 \text{scenario}}$ equals the mean of $T_{2\times CO_2}$, this being a desirable property of the estimator of future temperature. The scaling ratios and differences shown in equations (3) and (4), respectively, represent averages computed from several GCM/RCM outputs for regions within the conterminous United States. Loáiciga *et al* (2000) and Loáiciga (2003) used precipitation ratios and temperature differences to drive a hydrologic model of runoff production from which recharge (by stream seepage) was calculated. A similar approach underlies the results presented in a section 4.2 of this paper dealing with global warming scenarios and spring flow response. The reader is referred to Wilby and Wigley (1997) for a review of climatic downscaling methods.

There are strong assumptions underlying the accuracy of future climate scenarios using the scaling ratios and temperature differences embodied in equations (3) and (4), respectively. It is assumed, for example, that historical climatic variables scale proportionally or shift linearly with respect to the ratios or differences, respectively. Also, the timing of events such as droughts and floods follows the same pattern observed historically. That is why this method of scaling and shifting is best suited to attempt to predict climate scenarios under below-normal precipitation (droughts), or normal precipitation, or above-normal precipitation, where the differences among extremes and averages are highlighted in the climate scenarios so created. It cannot be overlooked either that the use of ratios and differences of $1 \times CO_2$ and $2 \times CO_2$ neglects the transient rise of atmospheric CO_2 over a span of time 100 years long. In spite of the limitations of

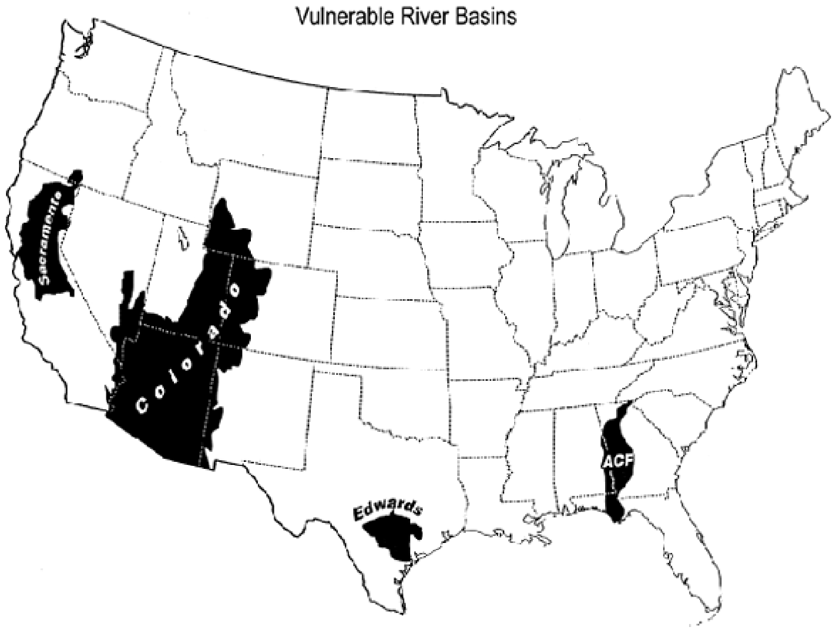

Figure 10. River basins vulnerable to climate change in the United States (after Loáiciga *et al* 1998).

the scaling/shifting approach herein used, the alternative, or transient GCM simulations of the future climate, are fraught with their own limitations (IPCC 2007). Both steady-state and transient simulations of the future climate are beset by the current imperfect knowledge of factors governing climate change (such as modifications in planetary albedo, atmospheric transmissivity, air moisture, oceanic circulation, ice melting) and related nonlinear feedbacks (Loáiciga *et al* 1996, Loáiciga 2003, Roe and Baker 2007). In spite of the cited limitations, one must acknowledge the steady progress made over the last two decades in our capacity to simulate numerically the world's climate. The IPCC (2007) report summarizes several state-of-art models for climate prediction currently available. In the realm of climate prediction and water resources impacts, the papers by Scibek and Allen (2006), Serrat-Capdevila *et al* (2007), Fowler *et al* (2007) are exemplary.

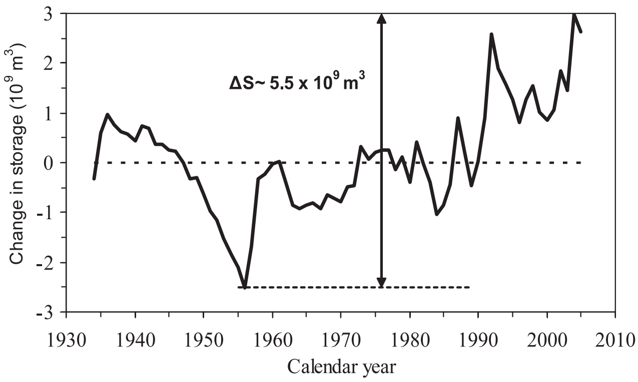

Figure 11. Change in storage in the Edwards aquifer with estimated storage capacity ΔS. (Source: Edwards aquifer authority, San Antonio, Texas; Loáiciga 2008.)

4. Groundwater management in a warmer world

4.1. Historical hydrologic records: inter-annual variability and stationarity

One of the most productive aquifers in the United States is the Edwards aquifer of south-central Texas, which provides water for economic, urban, and environmental needs in greater San Antonio, Texas and its environs. The approximate geographical layout of the Edwards aquifer is shown in figure 10, where it is shown with other river basins deemed vulnerable to current climate change (Loáiciga *et al* 2000, Loáiciga 2002). Vulnerable in this context is synonymous to highly probable deleterious changes in water quantity and quality that threaten society, ecosystems or water-dependent habitats. Extending over 6109 km^2 of recharge and discharge area, the Edwards aquifer is made up of karstified carbonate rocks of high transmissivity. A hydrogeologic description of the Edwards aquifer is found in Loáiciga *et al* (2000), Loáiciga (2003), (2008), which also examined the vulnerability of its spring flow to global warming.

The storage capacity of the Edwards aquifer is illustrated by figure 11, which shows the annual change in aquifer storage from 1934 though 2007 (adapted from Loáiciga 2008). Notice the persistence of low storage between 1947 and 1959, the period of critical drought. The difference between maximum and minimum change of storage suggests that the aquifer storage capacity is at least 5.5×10^9 m^3.

Figure 12 shows time series of annual precipitation (P) and recharge (R) into the Edwards aquifer from 1934 through 2007. Five year moving averages for these time series (P-5, R-5) are also shown on figure 12. The recharge data show low levels between 1947 and 1956, this being within the critical drought period (1947–1959). Recharge is calculated by water balancing in the recharge area of the aquifer according to a

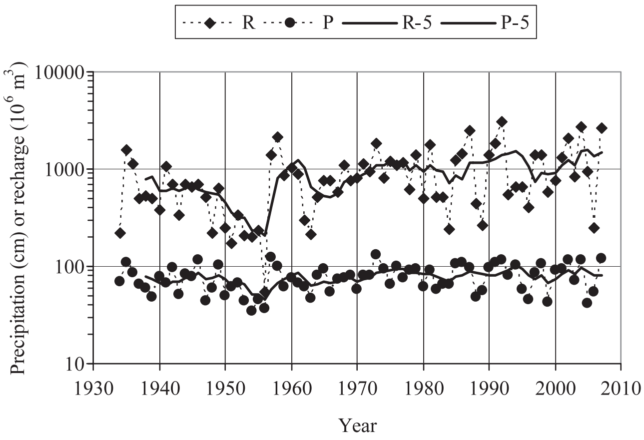

Figure 12. Annual precipitation (P), recharge (R), and 5 year moving averages (P-5, R-5) in the Edwards aquifer, 1934–2007. (Source: Edwards aquifer authority, San Antonio, Texas.)

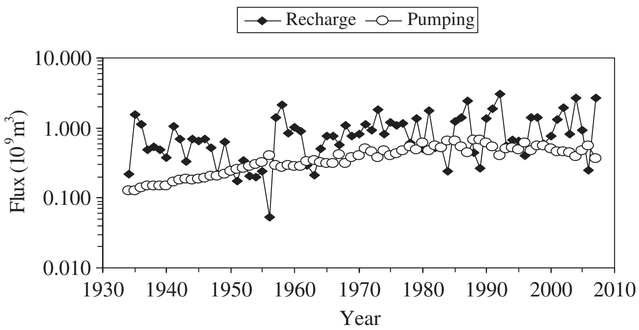

Figure 13. Annual recharge and ground water pumping in the Edwards aquifer (in 10^9 m^3), 1934–2007. (Source: Edwards aquifer authority, San Antonio, Texas).

method by Puente (1978). The precipitation and recharge time series do not exhibit any long-term trends. Their inter-annual variability is pronounced. These high-quality data establish that global warming trends do not appear to have modified either recharge or precipitation in the Edwards aquifer during the last seven decades.

Figure 13 shows the annual time series of recharge and ground water pumping in the Edwards aquifer from 1934 to 2007.

Unlike recharge, the ground water pumping data in figure 13 exhibit an overall rising trend from 1934 through 1985. Lawsuits filed by environmental advocates prevented further increase of ground water pumping, which by 1980 had diminished spring flow to the point where several aquatic species had become threatened or endangered (Loáiciga *et al* 2000).

Figure 14 displays annual recharge data and spring flow data from 1934 to 2007.

It is seen in figure 14 there that spring flow was lowest during the drought period, and also in the period 1978–1991, which, although having had average recharge, exhibited high ground water pumping. The spring flow and ground water pumping data show that the human environmental footprint has grown over time.

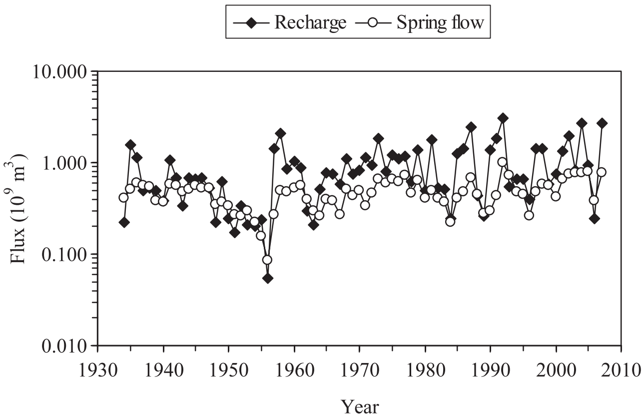

Figure 14. Annual recharge and spring flow in the Edwards aquifer, 1934–2007. (Source: Edwards aquifer authority, San Antonio, Texas.)

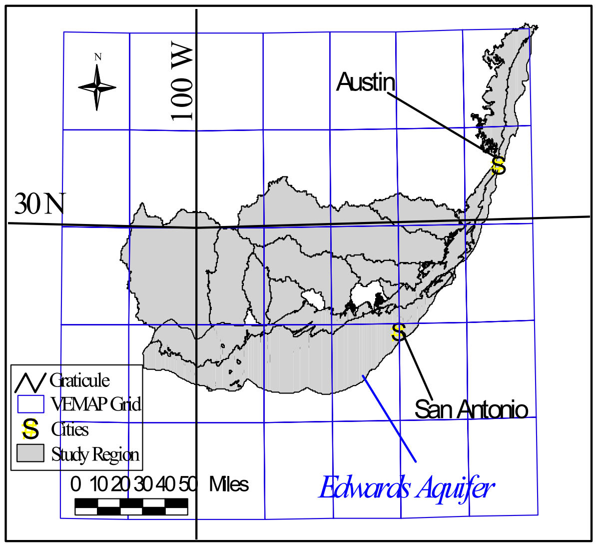

Figure 15. RCM spatial grid over the Edwards aquifer.

4.2. Global warming scenarios and spring flow response

The scaling-ratio approach embodied by equations (3) and (4) was used by Loáiciga *et al* (2000), Loáiciga (2003) to create recharge inputs to a ground water flow numerical simulation model. The ratios were obtained from the NCAR-VEMAP database cited above. These ratios represented averages over a spatial grid of a Regional Climate Model with cells 0.5° × 0.5° latitude/longitude in size within the Edward aquifer region, shown in figure 15.

The input recharge data was used to drive the regional ground water flow model GWSIMIV for the Edwards aquifer (Thorkildsen and McElhaney 1992). GWSIMIV calculates hydraulic head in each of its numerical grid cells and spring flow at selected cells where springs are located. The scaling procedure was implemented to create 2 × CO_2 recharge scenarios corresponding to average recharge (historical period 1978–1989) or drought (historical period 1947–1959) with which to drive the GWSIMIV model.

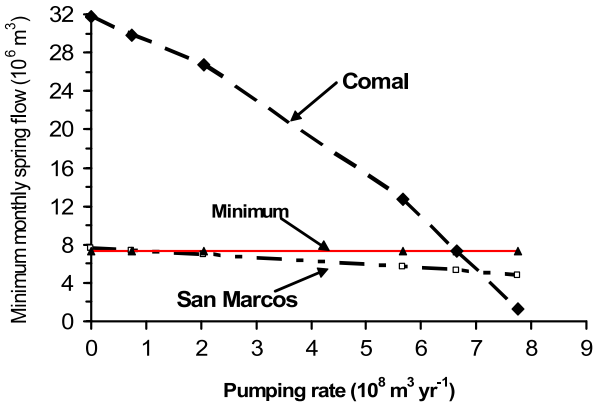

Figure 16. Calculated spring flow rates for average $2 \times CO_2$ recharge in the Edwards aquifer.

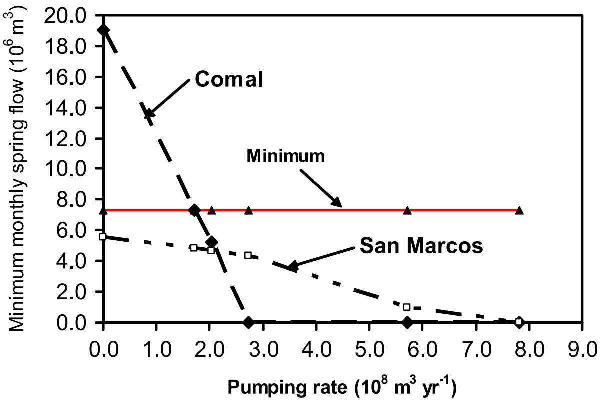

Figure 17. Calculated spring flows for $2 \times CO_2$ drought conditions in the Edwards aquifer.

Figure 16 (adjusted from Loáiciga *et al* 2000) shows the results for minimum spring flow in the two major springs in the Edwards aquifer, namely, the Comal and San Marcos Springs for $2 \times CO_2$ recharge constructed by scaling average historical recharge (period 1978–1989). The spring flows were calculated with the GWSIMIV model for a range of annual ground water pumping. The two springs exhibit drastically different responses to ground water pumping.

Comal spring flow crosses a recommended minimum spring flow threshold at about 6.8×10^8 m^3 year^{-1} of ground water pumping. San Marcos spring flow response is relatively insensitive to ground water pumping and decreases slowly with increasing ground water pumping. At 2×10^8 m^3 year^{-1} of ground water pumping the spring flow is slightly below the recommended minimum threshold. A plausible range of recommended ground water pumping for future average recharge could be 2.0×10^8–6.0×10^8 m^3 year^{-1}, given that the spring flows are close to the minimum threshold for this range of pumping.

Figure 17 (adjusted from Loáiciga *et al* 2000) shows similar information as that in figure 17 except that the $2 \times CO_2$ recharge was constructed by scaling drought historical recharge (period 1947–1959).

In this case Comal spring flow is below the minimum recommended threshold at 2×10^8 m^3 year^{-1}, while San Marcos spring flow is below the minimum threshold even for nil ground water pumping. The reduced spring flow and its impacts on aquatic ecosystems calls in this case for reduced ground water pumping compared to average recharge conditions, perhaps pumping in the range 0–2.0×10^8 m^3 year^{-1}. This reduced ground water pumping would require substitute water sources to make up for the shortfall in municipal, industrial, commercial, agricultural, and military supplies. A diversified system of water sources supplemented with conservation, water recycling (reclamation), and water pricing must be developed to provide adequate water during drought periods, and, with population growth, even during average recharge years.

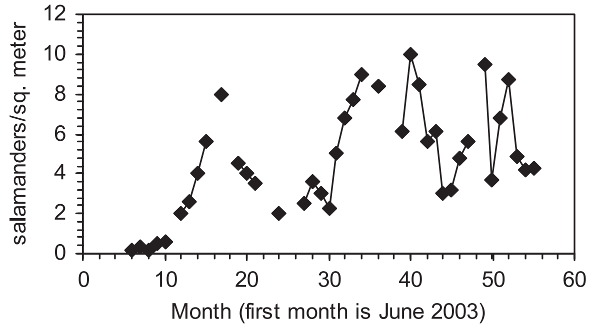

Figure 18. Change in salamander counts (*Eurycea sosorum*) in the Eliza spring, near the City of Austin, Texas (courtesy of Laurie Dries, 2008).

The importance of plentiful spring flow to support aquatic species is documented empirically. Figure 18 shows a plot of salamander counts (*Eurycea sosorum*) in the Eliza spring near the city of Austin, Texas, which is underlain by the Edwards aquifer. The salamander population viability was threatened by low spring flow in 2003. Spring flow recovery allowed the salamander population to rebound by mid 2005, after which its fluctuating numbers became a matter of natural seasonal variability, rather than human-induced reduction of spring flow.

4.3. Relative contributions of global warming and population growth to spring flow

The effect of global warming or climate change on spring flow is felt through changes in recharge. The effect of population growth is felt through increased ground water pumping. Let the function $f(Q, R)$ represent the response of spring flow to annual ground water pumping Q and annual recharge R. The total change in spring flow is then:

$$\Delta f = \frac{\partial f(Q, R)}{\partial Q}\Delta Q + \frac{\partial f(Q, R)}{\partial R}\Delta R. \quad (5)$$

The first term on the right-hand side of equation (5) represents the change in spring flow caused by a change in ground water pumping while the recharge is constant. The second term of the same right-hand side represents the change in hydrologic response (i.e., spring flow) caused by a change in recharge (a measure of a change in climate). The function $f(Q, R)$ is not known analytically. Therefore, one must approximate the right-hand side terms of equation (5) numerically. Loáiciga (2003) proposed an approximation whereby spring flows in the Edwards aquifer (using GWSIMIV numerical model) were calculated for four scenarios.

Scenario 1, the baseline: use average historical recharge (during period 1978–1989) and baseline ground water use (period 1978–1989).

Scenario 2, approximate climate-change impact alone: use average historical recharge scaled to $2 \times CO_2$ conditions using scaling-ratio approach, and baseline ground water use.

Scenario 3, approximate ground water use impact alone: use average historical recharge and year-2050 forecasted ground water use.

Scenario 4, approximate climate change and ground water use impacts combined: use average historical recharge scaled to $2 \times CO_2$ conditions and year-2050 forecasted ground water use.

The spring flow simulations for scenarios 1–4 revealed that:

(1) The climate-change scenario (scenario 2) increased spring flows at Comal and San Marcos springs by approximately 160% and 17%, respectively, relative to the baseline scenario (scenario 1).
(2) The ground water use impact scenario (scenario 3) decreased spring flows by 100% and 22% at Comal and San Marcos springs, respectively, relative to the baseline scenario.
(3) The ground water use impact and climate-change scenario (scenario 4) decreased spring flows by 73% and 1% at Comal and San Marcos springs, respectively, relative to the baseline scenario.

These results for scenarios 1–4 suggest the preponderance of the anthropogenic impact over the global warming impact (or climate-change impact) in the Edwards aquifer. This is a warning for those in charge for water supply and environmental planning in the Edwards aquifer region that a diversified water supply and conservation system must be developed to cope with increasing human water use and competing aquatic ecosystem requirements.

5. Summary

The heightened worldwide awareness concerning fossil-fuel use, the increase of GHGs in the atmosphere and their possible adverse climatic impacts, and about water resources impacts of global warming and population growth is timely and meritorious. This paper reviewed some of the difficulties clouding the prediction of regional effects of future climate change on water resources. To mitigate a somewhat daunting outlook in this respect, it also presented one approach to weigh the relative impacts of global warming and population growth in a very important regional aquifer of the United States. The results obtained concerning impacts of climate change and population growth in the Edwards aquifer in Texas are noteworthy and consistent with findings by this author in previous studies for various regions of the world (see Loáiciga *et al* 1996), and with global-scale studies by other authors (see Vörösmarty *et al* 2000), namely, that population growth will exert as great or greater an impact on the world's water resources as global warming might in the 21st century. The results obtained for the Edwards aquifer in this study and for other regional studies by this author (see Loáiciga and Renehan 1997) point to the need for water supply systems with diversified sources that can be tapped on under a variety of climatic conditions (wet, normal, dry), supplemented by sound conservation and water recycling programs that discourage waste.

A good example of a diversified water supply system is that of the City of Santa Barbara, California, where normally the largest (and cheapest) sources of water are regulated reservoirs. Ground water is tapped on as a supplement to reservoir water during long droughts. Ultimately, reservoir water and ground water failing, sea water desalination (the most expensive source) is activated during grave conditions of water scarcity.

The statements by Loáiciga *et al* (1996) about global warming and associated hydrologic-cycle issues are very pertinent today. First, the natural variability in regional hydrologic cycles is likely to dominate additional variability brought about by climate change in many regions of the world. Second, sound water resources engineering and management, with time-tested provisions for safety, ought to render water projects adequate with or without climate change. As for specifics on how to mitigate variability, change, and uncertainty, Klemes (1991) proposed guidelines to cope with future climate change in the context of water resources planning and design: (1) adherence to high professional standards in solving water resource problems, (2) commitment to measures limiting water waste and pollution, (3) striving for robust and resilient designs, (4) documenting and taking into account known uncertainties in water supply and demand, (5) documenting the ranges of feasible operation of projects, rather than providing only nominal design parameters, (6) providing a general outline of feasible contingency measures for extreme conditions not accommodated by the project under normal operation (i.e., flexible operating rules), and (7) insistence on clear disclosure of factual information, assumptions, and conjectures behind modeling results to be considered.

Lastly, this paper points to rapid and relentless population growth as one of the factors that deserves greatest attention in order to succeed in providing, adequately and timely, suitable water for society and the environment.

Acknowledgments

The work leading to this paper was supported in part the University of California's Water Resources Center, through grant WR-2007-09. The contents and ideas of this paper are the sole responsibility of its author and do not imply endorsement from the funding agency.

References

Arnell N W, Hudson D A and Jones R G 2003 Climate change scenarios from a regional climate model: estimating change in runoff in southern Africa *J. Geophys. Res.* **108** 4519–26

Barnett T P *et al* 2008 Human-induced changes in the hydrology of the Western United States *Science* **319** 1080–3
Berner R A 1997 The rise of plants and their effect on weathering and atmospheric CO_2 *Science* **312** 544–6
Budyko M 1977 *Climate Change* (Washington, DC: American Geophysical Union)
Cohen J E 1995 *How Many Can the Earth Support?* (New York: W W Norton)
Crowley J 2008 Overview of water/energy implications *Summary of Climate Change Implications for California Groundwater Management Symposium (California Groundwater Resources Association, Sacramento, California)*
de Witt M and Stankiewicz J 2006 Changes in surface water supply across Africa with predicted climate change *Science* **311** 1917–21
Duffy P B, Santer B D and Wigley T M L 2009 Solar variability does not explain late-20th-century warming *Phys. Today* **62** 48–9
Falkenmark M 1997 Meeting water requirements of an expanding world population *Phil. Trans. R. Soc.* **352** 929–36
Fedorov A V, Dekens P S, McCarthy M, Ravelo A C, de Menocal P B, Barreiro M, Pacanowski R C and Philander S G 2006 The Pliocene paradox: mechanisms for a permanent El Niño *Science* **312** 1485–9
Forest C E, Stone P H, Sokolov A P, Allen M R and Webster M D 2002 Quantifying uncertainties in climate system properties with the use of recent climate observations *Science* **295** 113–7
Fowler H J, Kilsby C G and Stunnel J 2007 Modeling the impact of future projected climate change on water resources in north-west England *Hydrol. Earth Syst. Sci.* **11** 1115–26
Gleick P 2004 *The World's Water 2004–2005: the Biennial Report on Freshwater Resources* (Washington, DC: Island Press)
Grassi H 2000 Status and improvements of coupled general circulation models *Science* **288** 1991–7
Gribbin J 1979 *Climatic Change* (Cambridge: Cambridge University Press)
Hansen J *et al* 2005 Earth's energy imbalance: confirmation and implications *Science* **308** 1431–4
Hardin G 1993 *Living within Limits: Ecology, Economics, and Population Taboos* (New York: Oxford University Press)
Houghton J 2004 *Global Warming* 3rd edn (Cambridge: Cambridge University Press)
Imbrie J and Imbrie J Z 1980 Modeling the climatic response to orbital variations *Science* **207** 943–53
IPCC (Intergovernmental Panel on Climate Change) 2007 *Climate Change 2007* vols I, II, III (Cambridge: Cambridge University Press) also available online at http://www.ipcc.ch
Kittel T G F, Rosenbloom N A, Painter T H and Schimel D S 1995 VEMAP modeling participants, the VEMAP integrated database for modeling United States/vegetation sensitivity to climate change *J. Biogeogr.* **22** 857–62
Klemes V 1991 Design implications of climate change *Proc. First National Conf. of Climate Change and Water Resources* ed T Ballentine and E Z Stakhiv (Washington, DC: US Army Corps of Engineers) pp III-9–19
Krauskopf K 1979 *Introduction to Geochemistry* 2nd edn (New York: McGraw-Hill)
Loáiciga H A 2002 Sustainable ground water exploitation *Int. Geol. Rev.* **44** 1115–21
Loáiciga H A 2003 Climate change and ground water *Ann. Assoc. Am. Geogr.* **93** 30–41
Loáiciga H A 2006 Modern-age buildup of CO_2 and its effects on seawater acidity and salinity *Geophys. Res. Lett.* **33** L10605
Loáiciga H A 2007 Reply to comment by K Caldeira *et al* on Modern-age buildup of CO_2 and its effects on seawater acidity and salinity *Geophys. Res. Lett.* **34** L18603
Loáiciga H A 2008 Aquifer storage capacity and maximum annual yield from long-term aquifer fluxes *Hydrogeol. J.* **16** 399–403
Lorenz E N 1964 The problem of deducing the climate from the governing equations *Tellus* **16** 1–11
Loáiciga H A, Maidment D and Valdes J B 1998 Climate change impacts on the water resources of the Edwards Balcones fault zone aquifer, Texas *Report ASCE/USEPA Cooperative Agreement CR 824540-01-0* (Washington, DC: US Environmental Protection Agency, Office of Policy)
Loáiciga H A, Maidment D and Valdes J B 2000 Climate change impacts in a regional karst aquifer, Texas, USA *J. Hydrol.* **227** 173–94
Loáiciga H A and Renehan S 1997 Municipal water use and water rates driven by severe drought: a case study *J. Am. Water Resources Assoc.* **33** 1313–26
Loáiciga H A, Valdes J B, Vogel R, Garvey J and Schwarz H 1996 Global warming and the hydrology cycle *J. Hydrol.* **174** 83–127
Milliman J D, Farnworth K L, Jones P D, Xu K H and Smith L C 2008 Climatic and anthropogenic factors affecting river discharge to the global ocean, 1951–2000 *Glob. Planet. Change* **62** 187–94
Oki T and Kane S 2006 Global hydrological cycles and world water resources *Science* **313** 1068–72
Pielke R Jr 2008 A broader view of the role of humans in the climate system *Phys. Today* **61** 54–5
Postel S L, Daily G C and Ehrlich P R 1996 Human appropriation of renewable fresh water *Science* **271** 785–8
Puente C 1978 A method of estimating natural recharge to the Edwards Aquifer in the San Antonio area, Texas *USGS Water Resources Investigations Report No. 78-10* 34 pages
Pugh D 2004 *Changing Sea Levels* (Cambridge: Cambridge University Press)
Roe G H and Baker M B 2007 Why is climate sensitivity so unpredictable *Science* **318** 629–32
Scafetta N and West B J 2008 Is climate sensitive to solar variability *Phys. Today* **61** 50–1
Scibek J and Allen D M 2006 Modeled impacts of predicted climate change on recharge and ground water levels *Water Resources Res.* **42** W11405
Serrat-Capdevila A, Valdés J B, González Pérez J, Baird K, Mata L J and Maddock T III 2007 Modeling climate change impacts and uncertainty on the hydrology of a riparian system: the San Pedro Basin (Arizona/Sonora) *J. Hydrol.* **347** 48–66
Shiklomanov J A and Rodda J 2003 *World Water Resources at the Beginning of the 21st Century* (Cambridge: Cambridge University Press)
Thorkildsen D and McElhaney P D 1992 Model refinement and applications for the Edwards BFZ aquifer in the San Antonio Region *Texas Water Development Board Report 340 (Austin, Texas)*
Tsonis A 1991 Sensitivity of the global climate system to initial conditions *EOS Trans. Am. Geophys. Union* **72** 313–28
Vörösmarty C J, Green P, Salisbury J and Lammers R B 2000 Global water resources: vulnerability from climate change and population growth *Science* **289** 284–8
Wilby R L and Wigley T M L 1997 Downscaling general circulation model output: a review of method and limitations *Prog. Phys. Geogr.* **21** 530–48